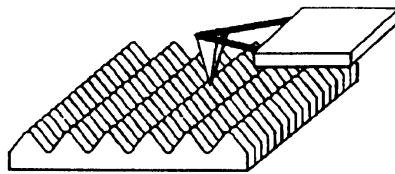


# Chemnitz University of Technology



## X. International Colloquium on Surfaces



## X. Internationales Oberflächenkolloquium

## Proceedings + Poster Vorträge + Poster

31st January to 2nd February  
of the Year 2000

Die Deutsche Bibliothek - CIP-Einheitsaufnahme

**X. International Colloquium on Surfaces - X. Internationales  
Oberflächenkolloquium, Chemnitz (Germany) Jan. 31 - Feb. 02, 2000:**  
Proceedings & Posters - Vorträge & Poster / M. Dietzsch, H. Trumpold (Hrsg.).  
- Als Ms. gedr. -  
Aachen: Shaker, 2000  
ISBN 3-8265-6999-7

Copyright Shaker Verlag 2000

Alle Rechte, auch das des auszugsweisen Nachdruckes, der auszugsweisen  
oder vollständigen Wiedergabe, der Speicherung in Datenverarbeitungs-  
anlagen und der Übersetzung, vorbehalten.

Als Manuskript gedruckt. Printed in Germany.

ISBN 3-8265-6999-7

Shaker Verlag GmbH • Postfach 1290 • 52013 Aachen  
Telefon: 02407 / 95 96 - 0 • Telefax: 02407 / 95 96 - 9  
Internet: [www.shaker.de](http://www.shaker.de) • eMail: [info@shaker.de](mailto:info@shaker.de)

# Highly accurate surface measurement by means of white light confocal microscopy

## Hochgenaue Oberflächenmessung mit Hilfe von konfokalen Weißlichttechniken

H.-J. Jordan (NanoFocus Messtechnik GmbH), R. Brodmann (Brodmann Marketing & Vertrieb)

### 1. Introduction

The technique of confocal microscopy, as first described by M. Minsky in 1957 as the so called double focusing microscopy [1, 2] becomes a more and more powerful tool for 3D characterisation of engineering surfaces.

In reflection mode confocal microscopy, light emitted from a point light source is imaged into the object focal plane of a microscope objective (the first focussing). A specimen location in focus leads to a maximum flux of the reflected light through a detector pinhole (the second focussing), whereas light from defocused object regions is partly suppressed. The depth discriminated detector signal, limited by the pinhole size, is reduced strongly when defocusing the specimen [3, 4]. This effects in optical sectioning and contrast enhancement by suppression of light scattered from defocused specimen locations and allows an accurate determination of the specimens  $z$  co-ordinate. A further advantage of confocal microscopy against classical light microscopy is an increase of the lateral resolution of about 20% [5].

Different designs of confocal microscopes are possible for the acquisition and evaluation of 3D topographic data. Time consuming serial  $xy$ -scanning techniques have been developed for the acquisition of depth discriminated sections in confocal laser scanning microscopes, a further  $z$ -scan is necessary to acquire all the data for the evaluation of 3D topographic maps [6, 7].

The NanoFocus™  $\mu$ Surf™ confocal microscope is using a multiple pinhole mask (Nipkow disk) in an intermediate image plane of a microscope as first described by Petran [8]. Combined with CCD image processing, the rotating Nipkow disk affects a real-time  $xy$ -scan of the object field. Just an additional  $z$ -scan is necessary for 3D acquisition [9, 10].

### 2. Theory of 3D confocal microscopy

A comprehensive description of the theory of confocal microscopy is given in [5], some formulas relevant for 3D topometry are as follows [9, 10]. The depth response  $I(z)$  of a confocal system is proportional to a  $SINC^2$  function,

$$I(z) = \left( \frac{\sin(kz(1 - \cos a))}{kz(1 - \cos a)} \right)^2 I_0 \quad (1)$$

which is depending on the aperture angle  $a$  of the microscope objective, the wavelength of light  $\lambda$ , the wavenumber  $k = 2\pi/\lambda$  and the co-ordinate of defocusing  $z$ . Significant for the depth response  $I(z)$  is the Full Width at Half Maximum, which is

$$FWHM = 2 z_{1/2} \approx \frac{0,443 \lambda}{1 - \cos a} \quad (2)$$

The half angle of the numerical aperture  $NA$  determines the maximum surface slope

$$a_{\max}^{spec} = 0.5 \sin^{-1} NA \quad (3)$$

for specular reflection at a microscopic smooth surface element of the specimen. The wavelength together with the numerical aperture determine the full width at half maximum *FWHM* of the depth response  $I(z)$  of the detectors intensity.

Engineering surfaces often have micro-roughness within the probe spot size, therefore diffuse reflection increases the maximum surface slope which can be measured ( $a^{diff} \geq a_{max}^{spec}$ ) and  $a_{max}^{spec}$  according to equation 3 indicates a lower limit of the surface slope.

### 3. The NanoFocus™ $\mu$ Surf™ 3D confocal microscope

The  $\mu$ Surf™ measurement station (figure 1) consists of a compact confocal module, which includes all the optics. An external Xenon lamp is connected to the confocal module via a light guide. The confocal module is fixed on the precise stepper motor driven linear axis which is mounted on a solid bridge stand. The sample is placed on an  $xy$  precision slide. For a non-contact measurement of surface topography the sample is positioned using the  $xy$  precision slide and the confocal module is moved stepwise in  $z$ -direction (Piezo with 100 $\mu$ m travel and 10nm resolution or precise stepper motor driven linear axis with 100mm travel and 100nm resolution). The NanoFocus™  $\mu$ Surf™ confocal microscope is controlled by software running under Microsoft™ Windows™ (95 / 98 / NT4.0). The surface topographic data can be visualised and analysed in various ways.

For  $xy$ -scanning of a depth discriminated section we use a Nipkow disk, which consists of an array of pinholes arranged in a spiral shape. The rotating disk is illuminated by a plane wave and acts as a scanning multiple point light source, which is imaged into the object focal plane of the microscope objective. After the reflection of light, each illuminating Nipkow pinhole acts as his own detector pinhole. The depth discriminated  $xy$  information  $I(x,y,z)$  is imaged onto a CCD camera. Thus, during one rotation of the disk, a  $xy$ -section of the specimen is acquired in video real-time. Image processing and height evaluation is done using a 512  $\times$  512 pixel frame-grabber.

By an additional  $z$ -scan of the specimen, a stack  $z_1$  to  $z_n$  ( $n < 3000$ ) of depth discriminated CCD camera-frames is acquired, from which a 3D topography can be constructed with an resolution of about 1% of the *FWHM*. In figure 2, a measured depth response  $I(x_i, y_j, z)$  and the mode of evaluation of the height coordinate  $h(x_i, y_j)$  as the centre of  $I(x_i, y_j, z)$  is presented. A well formed depth response according to the equations 1 and 2 is decisive for accurate confocal 3D topometry. Technical data of the  $\mu$ Surf™ are summarised in Table 1.



**Fig. 1:** The  $\mu$ Surf™ measurement station

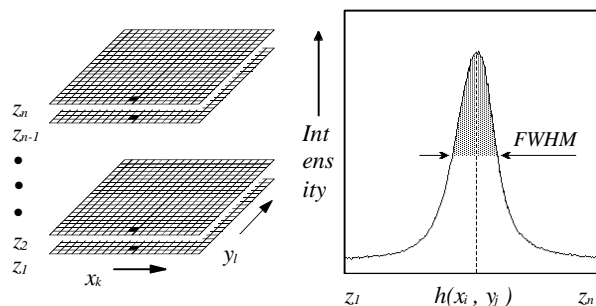


**Fig. 2:** The evaluation of the topography: Calculation of the height co-ordinate  $h(x_i, y_j)$  as the centre of the depth response  $I(x_i, y_j, z)$  for each pixel of the stack  $z_1$  to  $z_n$ .

Microscope objective	10x	20x	50x	100x
Basic field [ $\mu\text{m} \times \mu\text{m}$ ]	1600 x 1510	800 x 755	320 x 302	160 x 151
Working distance [mm]	10,1	3,1 / 12,0*	0,66 / 10,6*	0,31 / 3,4*
Numerical aperture	0,30	0,46 / 0,40*	0,80 / 0,50*	0,95 / 0,80*
Max. slope for specular reflection [deg.]	8,7	13,7 / 11,7*	26,6 / 15,0*	35,9 / 26,6*
Vertical resolution	50	<30 / <20**	<20 / <10**	<20 / <5**

**Table 1: Technical data of the  $\mu\text{Surf}^{\text{TM}}$ .**

\* Long working distance  
 \*\* Piezo for high resolution

The accuracy of the  $\mu\text{Surf}^{\text{TM}}$  measurement principle have been approved in all 3 coordinates using several standards like the PTB depth setting or the PTB roughness standards [9, 10]. In former comparisons to tactile instruments a very good agreement not only in the profile records but also in roughness parameters was obtained [9, 10].

Based on the high accuracy of the  $\mu\text{Surf}^{\text{TM}}$  topographic data, a very powerful and effective stitching has been developed in order to overcome the limitation of the single measurement field size. For stitching, a set of single measurements with an field overlap between neighboured measurements of about 10% of the single measurement field size were acquired and combined using a correlation algorithm, which works in all 3 axis. A measurement result of this stitching is shown in the next section. It should be noticed that all presentations within this paper are showing raw data of the  $\mu\text{Surf}^{\text{TM}}$  system. No artefacts or spikes have been filtered out in any plot.

## 4. Experimental results using the NanoFocus<sup>TM</sup> $\mu\text{Surf}^{\text{TM}}$

### 4.1 LASERTEX sheet metal

Using the  $\mu\text{Surf}^{\text{TM}}$  stitching, the measurement field size can be increased without loss of resolution. Thus, stitching allows one to obtain measurement fields with high spatial and vertical resolution, which are big enough for example for roughness analysis according to the DIN requirements. The principle is demonstrated in figure 3, using a LASERTEX sheet. This specimen shows roughness as well as a complex form. Although this specimen has very steep slopes (up to 65 degrees), the back-scattered light - due to the micro-roughness of highest spatial frequencies - was sufficient for accurate data acquisition.

After the procedure as demonstrated in figure 3, the elimination of tilts is done using a height correlation in order to obtain the final result. As an example, a resulting topography of a 4x4 stitching for the LASERTEX sheet shown in figure 4, a profile evaluated from this topography is shown in figure 3

Up to 10x10 stitching on sheet metals have successfully been performed, the resulting topographies included about 16 million data points.

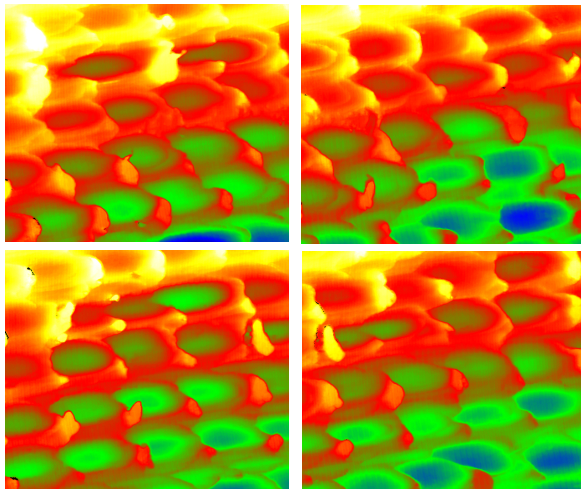
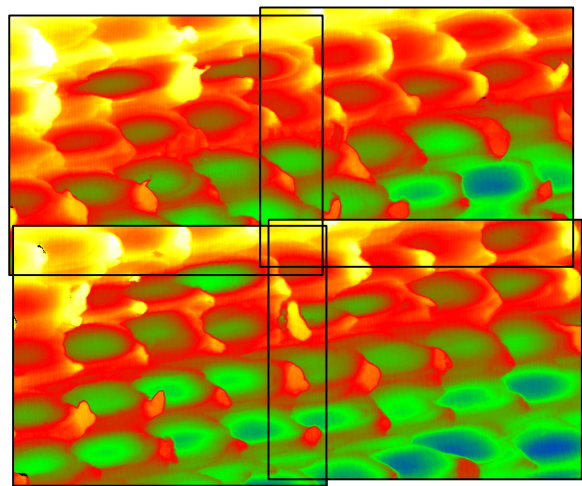


**Fig. 3:** An example of a 2x2  $\mu$ Surf™ stitching.  
*Left:* 4 single measurements, each with an overlap of about 10% to the neighbored one.



*Right:* In a first step, a stitching of patterns eliminates all possible positioning errors of the xy-stages.

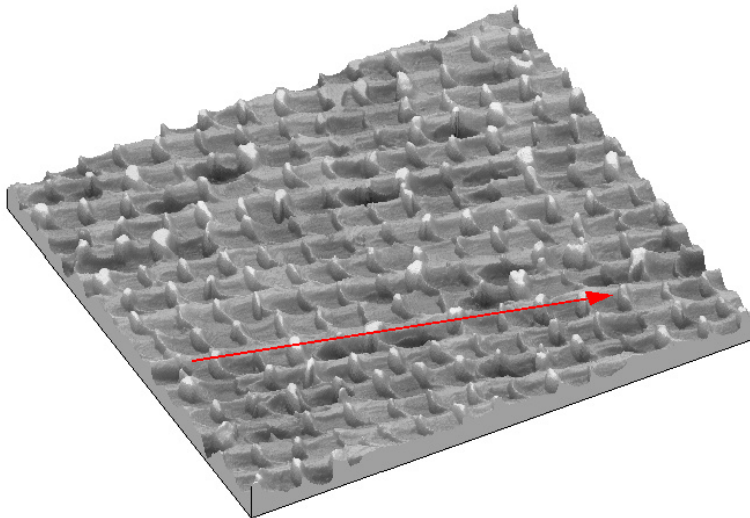


**Fig. 4:**

Topography of the LASER-TEX sheet, obtained by 4x4 stitching using the 20x objective.

Area: 2.3mm x 2.1mm  
 PV height: 12 $\mu$ m

Number of data points:  
 1726 x 1674  $\approx$  2.89 million.

The location of the profile from figure 5 is also shown.

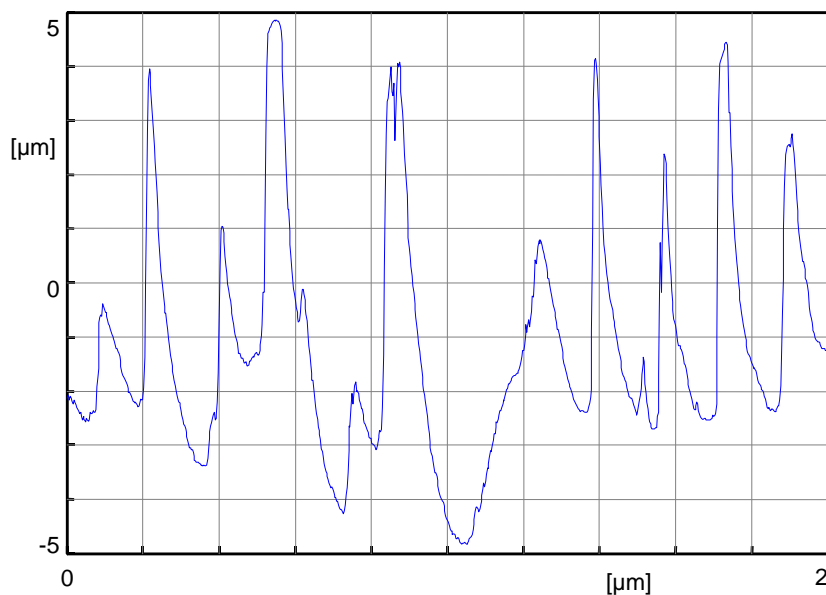


**Fig. 5:**

Profile as indicated in figure 4.

Profile length: 2mm  
 Vertical plot range: 10 $\mu$ m

## 4.2 MEMs

One of the strengths of the  $\mu\text{Surf}^{\text{TM}}$  instrument is the 3D topometry of sharp edges and high aspect ratios as they appear for example in LIGA structures. Figure 6 shows a 3D data set in grey-scaled top of view presentation, figure 7 a short profile with its location as indicated in figure 6.

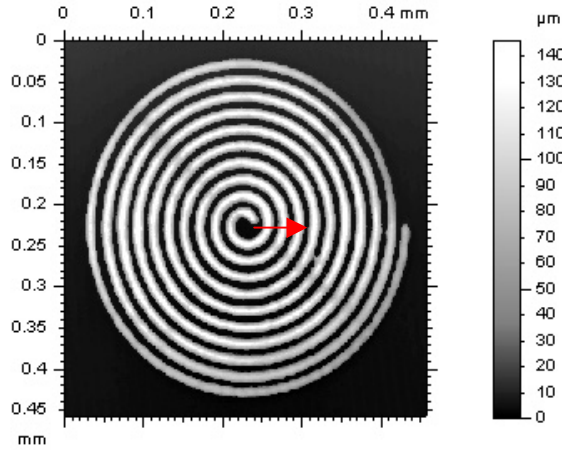


**Fig. 6:** 3D data set of a spiral produced in LIGA technique. The height of the spiral is  $\approx 140\mu\text{m}$ . The area is  $\approx 470\mu\text{m} \times 470\mu\text{m}$ . The location of the profile from figure 7 is also shown.

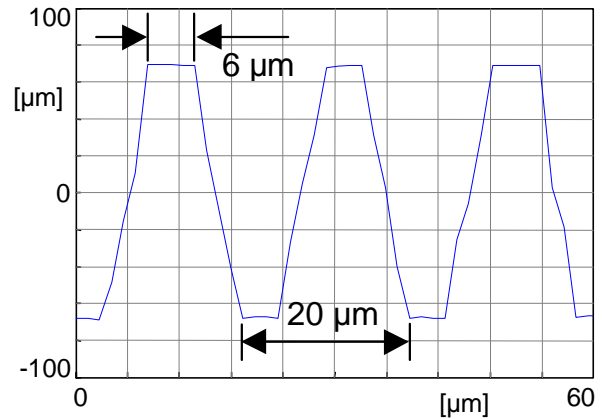


**Fig. 7:** A profile of  $60\mu\text{m}$  length as indicated in figure 6. Measured data are: Top bar width  $\approx 6\mu\text{m}$ , period  $\approx 20\mu\text{m}$ , edge slope  $\approx 88$  degree.

The aspect ratio (structure height divided by structure period) is in the order of 7. Again as mentioned above, this figures are presentations of raw data. No artefacts or spikes have been filtered out in this plots, although the edge slope exceeds the theoretical measurable slope  $a_{\text{max}}^{\text{spec}}$  (equation 3) for specular reflection dramatically and the edge slope covers 4 pixels. This coherence still has to be investigated in future.

## 4.3 Abrasive materials

Another example for analysis of complex surfaces using the  $\mu\text{Surf}^{\text{TM}}$  instrument is the 3D topometry of abrasive materials.

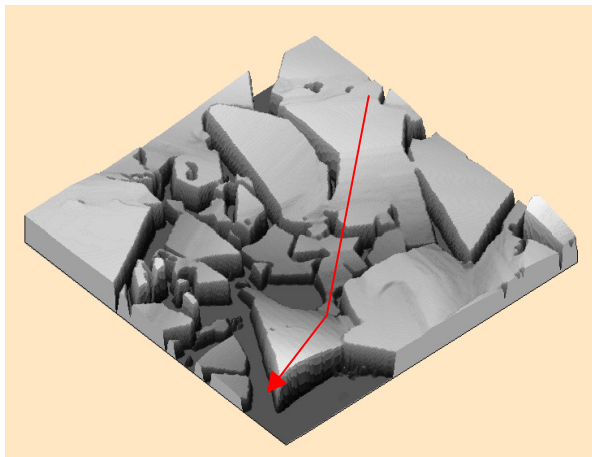


**Fig. 8:** 3D data set of a diamond abrasive paper. The area is  $280\mu\text{m} \times 280\mu\text{m}$  ( $50\times$  objective). The PV height is  $44.8\mu\text{m}$ . The location of the profile from figure 9 is also shown.

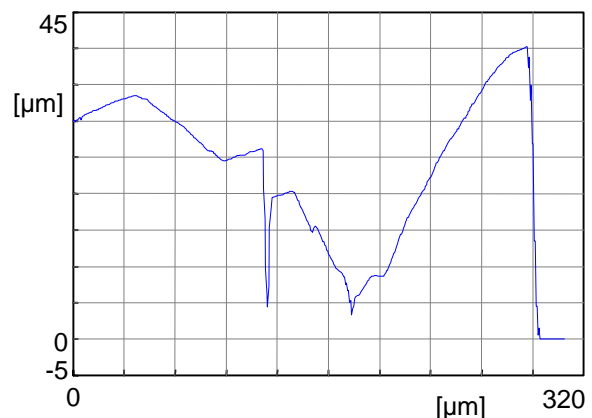


**Fig. 9:** A profile of  $320\mu\text{m}$  length, as indicated in figure 4.

Figure 8 shows a 3D data set of diamond abrasive paper in grey-scaled isometric projection, figure 9 a profile with its location as indicated in figure 8. This sample is composed of splits of diamonds with arbitrary size, shape and orientation. Thus, the topography contains a lot of unsteadiness in the topographic height, as can be seen in the profile of figure 9.

#### 4.4 More applications

The NanoFocus™  $\mu$ Surf™ confocal microscope is capable for accurate measurement of a big variety of surface types like roughness, form and wear analysis of metallic and ceramic surfaces, form measurement and defect analysis of MEMs (Masters and replicates in semiconductors, LIGA, PMMA, photoresist or other techniques), form and roughness of cutting tools and others.

### 5. Conclusions

The NanoFocus™  $\mu$ Surf™ is a powerful instrument for fast and highly accurate non-contact 3D surface characterisation. Using the stitching tool large object fields become possible, even for rough engineering surfaces. The results obtained - raw data topographies as well as surface statistics - compare very well to tactile standard techniques. Thus, the  $\mu$ Surf™ is an powerful alternative to tactile techniques.

The images in figures 4, 6 and 8 have been produced using the MountainsMap™ software from Digital Surf™.

### 6. References

- [1] Minsky M., "Microscopy Apparatus", U.S. Patent 3013467 (19 Dec. 1961, filed 7 November 1957)
- [2] Minsky M., "Memoir on Inventing the Confocal Scanning Microscope", *Scanning* 10(4), 128-138 (1988)
- [3] Hamilton D. K., Wilson T., and Sheppard C. J. R., "Experimental observation of the depth-discrimination properties of scanning microscopes", *Opt. Lett.* 6 No 12, 625 (1981)
- [4] Wilson T., "Depth response of scanning microscopes", *Optik* 81 No 3, 113 (1989)
- [5] Wilson T., *Confocal Microscopy*, Academic Press, 1990
- [6] Hamilton D. K. and Wilson T., "Three-dimensional Surface Measurement using the confocal scanning microscope", *Appl. Phys. B* 27, 211 (1982)
- [7] Carlsson K. and Åslund N., "Confocal imaging for 3-D digital microscopy", *Appl. Opt.* 26 No 16, 3232 (1987)
- [8] Petran M., Hadravsky M., Egger M. D. and Galambos R., "Tandem-Scanning Reflected-Light Microscope", *J. Opt. Soc. Am.* 58(5), 661 (1968)
- [9] Jordan H.-J., Wegner M., and Tiziani H., "Optical topometry for roughness measurement and form analysis of engineering surfaces using confocal microscopy", in *Progress in Precision Engineering and Nanotechnology*, Proceedings of the 9th International Precision Engineering Seminar / 4th International Conference on Ultraprecision in Manufacturing Engineering, ISBN 3-9801433-9-2, (1997)
- [10] Jordan H.-J., Wegner M., and Tiziani H., "Highly accurate non-contact characterisation of engineering surfaces using confocal microscopy", *Meas. Sci. Technol.* 9, 1142-1151 (1998)

**The X. International Colloquium on Surfaces  
was supported by the following institutions**

International Institution for Production  
Engineering Research (CIRP)



Deutsches Institut für Normung e.V. (DIN)  
Normenausschuß Länge u. Gestalt (NLG)



Deutsche Forschungsgemeinschaft (DFG)



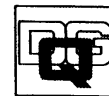
Stiftung zur Förderung der Forschung  
für die gewerbliche Wirtschaft



VDI/VDE Gesellschaft Meß- und  
Automatisierungstechnik (GMA)



Deutsche Gesellschaft für Qualität (DGQ)  
Frankfurt/M.  
Regionalkreis Chemnitz



Sparkasse Chemnitz



Gesellschaft der Freunde der  
Technischen Universität Chemnitz e.V.



GFMeßtechnik GmbH, Teltow



Taylor Hobson GmbH, Wiesbaden



Hommelwerke GmbH,  
Villingen-Schwenningen



Mitutoyo Meßgeräte GmbH, Neuss



Mahr GmbH, Göttingen



Carl Zeiss Meßtechnik, Oberkochen



Gesellschaft für angewandte technische  
optische Systeme mbH, Pfungstadt

